Interrelating of ventricular pressure and intracellular calcium in intact hearts

DAVID BARAN,[1] KAZUHIDE OGINO,[1] RICHARD STENNETT,[2]
MATTHEW SCHNELLBACHER,[1] DONNA ZWAS,[3]
JAMES P. MORGAN,[4] AND DANIEL BURKHOFF[1]
[1]*Department of Medicine, Columbia-Presbyterian Medical Center, New York 10032;*
Departments of [2]*Anesthesiology and* [3]*Medicine, New York Hospital, New York 10021; and*
[4]*Department of Medicine, Beth Israel Hospital, Boston, Massachusetts 02215*

Baran, David, Kazuhide Ogino, Richard Stennett, Matthew Schnellbacher, Donna Zwas, James P. Morgan, and Daniel Burkhoff. Interrelating of ventricular pressure and intracellular calcium in intact hearts. *Am. J. Physiol.* 273 (*Heart Circ. Physiol.* 42): H1509–H1522, 1997.— Although the mechanistic link between variations in intracellular calcium and its effects on myofilament regulatory proteins and subsequent impact on cardiac muscle force production have been known for some time, characterization of cardiac contractile properties are predominantly confined to phenomenological descriptions of the relationship between either muscle length and force or ventricular pressure and volume. However, as recognition of the limitations of these theories grow, investigators have begun to look toward more fundamental theories of cardiac contraction to explain whole heart function. The goal of the present study was first to explore, on a theoretical level, the degree of complexity required in a biochemical model necessary to adequately explain both equilibrium and twitch contraction behavior of cardiac muscle. Central to this analysis was a critical examination of the evidence for and against the importance of a calcium-free, force-generating state. Next, we determined whether such theories can actually account for the interrelationships between the experimentally measured time courses of pressure generation and the calcium transient measured from intact ventricles during both normal twitches as well as during complex contraction sequences. The results of this analysis provide strong support for a four-state model, including the calcium-free, force-generating state. These results will help guide the continuing quest for a mechanistic theory of ventricular function.

aequorin; ventricular mechanics; cross-bridge kinetics; excitation-contraction coupling

THE MYOCARDIUM CONTRACTS rhythmically in response to cyclic release and sequestration of calcium. Although the mechanistic link between variations in intracellular calcium and its effects on myofilament regulatory proteins and subsequent impact on muscle force production have been known for some time (16), experimental characterization of cardiac contractile properties have largely been confined to phenomenological descriptions of the relationship between either muscle length and force (30) or ventricular pressure and volume (28, 29). However, as recognition of the limitations of these theories grows, investigators (7, 9, 17, 20, 23, 34) have begun to look toward more fundamental theories of cardiac contraction to explain whole heart function.

The focus of previous efforts in this realm (7, 17, 20, 23) has been to test the feasibility of various models of calcium-cross-bridge interactions by demonstrating that such theories can reproduce a plethora of contractile and metabolic phenomena observed in previous experiments on cardiac tissues and in the intact heart. For the most part, these studies have focused on the ability to explain either the equilibrium stress-strain-calcium interrelationships (i.e., during states of steady activation) or the dynamic aspects of these interrelationships such as would pertain during normal twitch conditions. However, there has been relatively little direct experimental validation that these theories can, in fact, be used to explain contractile behavior on a quantitative basis in either intact muscle or the whole heart.

Common to many of the theories being investigated is an underlying four-state model of cross-bridge interactions with calcium (5, 7, 13, 27, 34). These theories, which have seven or more adjustable rate constants, have a large number of degrees of freedom, which increases the chances that they can explain observed phenomena without necessarily relating to events occurring on the cellular level. It is, therefore, pertinent to ask whether simpler models with fewer degrees of freedom are sufficient to explain the phenomenology of cardiac contraction. The relevance of this question is highlighted by the fact that the dynamics of skeletal muscle contraction are well described by a simpler three-state model (31).

The goal of the present study was twofold. First, we explored, on a theoretical level, the degree of complexity required in a biochemical model necessary to adequately explain both equilibrium and twitch contraction behavior of cardiac muscle. Central to this analysis was a critical examination of the evidence for and against the importance of a calcium-free, force-generating state (27, 34). Next, we determined whether such theories can actually account for the interrelationships between the time courses of pressure generation and the calcium transient measured from intact ventricles during both normal twitches as well as during complex contraction sequences. The results of this analysis provide strong support for the four-state model and, accordingly, will help guide ongoing efforts to develop a mechanistic theory of ventricular contraction.

METHODS

Theoretical Considerations

The first part of the present study is a theoretical investigation of whether a four-state model of cross-bridge and calcium interactions is required to explain cardiac muscle mechanics

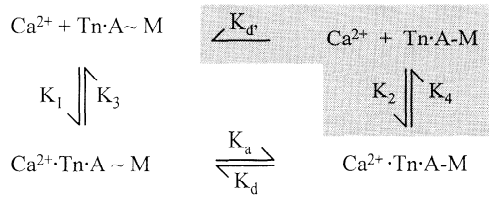

Fig. 1. Schematic representation of biochemical models proposed to account for interactions between calcium and myofilaments and force generation. Four-state model includes all components represented, whereas *state 4* and associated rate constants (gray area) are excluded in three-state model. Tn, calcium-binding subunit of troponin; A, actin; M, myosin; K_1, K_2, K_3, and K_4, calcium-binding affinities (rate constants) for *states 1–4*, respectively; K_a, association constant (actin-myosin affinity); K_d, dissociation constant for *state 3*; K_d', dissociation constant for *state 4*; ~, weak (nonforce-generating) bond; -, strong (force-generating) bond.

under equilibrium and twitch conditions or whether simpler models are sufficient. To accomplish this, we examined the behavior of four biochemical schemes based on the model topology depicted in Fig. 1. The most general model was a four-state model (which includes all elements in Fig. 1) with seven rate constants and a simpler three-state model (excluding elements in the gray area) with only four rate constants. In addition to examining the behavior of these two models with static rate constants, cooperativity was introduced into each model by making rate-constant values a function of product concentrations as detailed further below.

For all models, actin-myosin binding was considered to exist in two forms (13): a weak, nonforce-generating bond (Fig. 1, ~) and a strong, force-generating bond (Fig. 1, -). The physiological difference between the two models is that, in the four-state model, calcium can become dissociated from troponin (Tn) C with persistence of the strong actin-myosin bond (*state 4*), whereas in the three-state model, the strong bond (and therefore force production) can exist only in the presence of bound calcium. A major physiological question is how and the degree to which *state 4* contributes to the physiology of cardiac muscle contraction. The importance of addressing the relevance of *state 4* is highlighted by the fact that, for skeletal muscle, a similar analysis revealed that the simpler three-state model was able to predict the time course of force production from a measured calcium transient just as well as the four-state model, suggesting that *state 4* may not be important for skeletal muscle physiology (31). In contrast, it has been argued along several lines that the four-state model is required to explain several aspects of cardiac muscle physiology (detailed further below).

The set of differential equations describing each model is summarized in the APPENDIX. These were programmed on a digital computer for numerical solution as described in detail previously (7). The total concentrations of actin and myosin were set at previously established values (70 and 20 μM, respectively) (27). The output of the model was the instantaneous isometric muscle force or isovolumic pressure, both of which were assumed to be proportional to the concentration of strong actin-myosin bonds; for the four-state model, this was proportional to the total concentration of actin (A) bound to myosin (M) with a strong bond ([Ca^{2+}·Tn·A-M] + [Tn·A-M]), whereas in the three-state model, this was proportional to [Ca^{2+}·Tn·A-M]. Values of force were expressed in either micromoles of strong bonds or unitless, normalized values. The driving function for the equations was the instantaneous calcium concentration that could take on one of two forms. First, to explore equilibrium conditions, calcium was set at a fixed value, and the differential equations were allowed to settle at a steady value of force. After the force at a particular steady concentration of calcium was determined, the simulated calcium concentration was varied to a new value; the procedure was repeated until an entire equilibrium force-calcium curve could be constructed. The second type of calcium-driving function used was a typical time-varying function observed during a twitch. For this, we primarily used, as in a previous study (7), a previously published calcium transient determined from microinjected aequorin, for which a simultaneously recorded high-fidelity isometric-force tracing was also available (34) (Fig. 2). Values for the rate constants of each model were set to provide a good fit to both experimentally measured steady-state force-calcium curves and the force curve measured during the prototypical twitch; these values were in good agreement with those used by other investigators and in previous studies (7, 27). In view of the fact that calcium transients measured with different calcium indicators have slightly different characteristics, particularly during late diastole, we also performed a subset of the analyses based on another previously published calcium transient that was measured with fura 2 (2).

To determine whether the calcium-free, force-generating state was required to adequately describe cardiac muscle contractile properties, three- and four-state model muscles were subjected to several simulated physiological perturbations under steady-state and twitch conditions to determine whether any properties emerged that could distinguish the two models from each other. The details of these various perturbations are described in RESULTS.

As noted above, varying degrees of myofilament cooperativity were introduced into both of these models to test the impact of this important aspect of cross-bridge properties on the relationship between calcium and force production during twitch contractions. Hill coefficients relating the steady-state force-calcium binding curves are ~1.1 and 1.5 for the three-

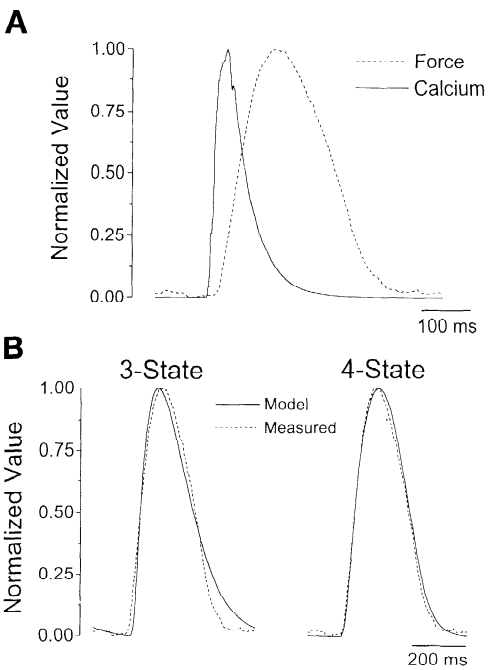

Fig. 2. *A*: normalized force and filtered calcium signals measured in isolated muscle strip by Yue (34). *B*: 3- and 4-state predictions of force (with optimally adjusted rate constants). Four-state model provides a marginally better fit to measured force curve overall, with most significant difference being evident during relaxation. See text for further details.

and four-state models, respectively, with no special cooperative mechanisms introduced. However, experimental studies have shown typical Hill coefficients ranging between 4 and 6 for intact preparations (1, 9, 11, 32, 35). In accordance with experimental observations showing that calcium binding affinity is enhanced by force production (6, 14, 17, 18), cooperativity was modeled by assuming that the calcium binding affinity of the myofilaments (K_1; rate constant) and the association constant (K_a; actin-myosin affinity) varied with the number of "strong" actin-myosin bonds. Other possible means of introducing cooperativity, including interactions based on the rate constants K_2, K_3, and K_4 for *states 2–4*, respectively, were studied individually as well as in combination, and these failed to produce reasonable Hill coefficients with acceptable fits to experimentally observed force tracings; the results obtained in those exercises will not be discussed further. To achieve varying amounts of cooperativity, K_1 and K_a were varied according to the following functions of actin-myosin strong bonds

$$K_1(t) = \alpha_1[[Ca^{2+}\cdot Tn\cdot A\text{-}M](t) + [Tn\cdot A\text{-}M](t)]^{\gamma_1} + \beta_1$$
$$K_a(t) = \alpha_a[[Ca^{2+}\cdot Tn\cdot A\text{-}M](t) + [Tn\cdot A\text{-}M](t)]^{\gamma_a} + \beta_a \quad (1)$$

where t is time, α and β are adjustable constants, and γ_1 and γ_a are constants set at 0.5 and 2.0, respectively, after sequential simulations showed that these values provided Hill coefficients ranging between 2 and 6 while also maintaining the ability to closely fit experimentally obtained force tracings. We next determined values of α and β that yielded Hill coefficients of ~2, 4, and 6 [while maintaining calcium for half-maximal activation (K_{50}) constant], and, finally, we assessed the impact of cooperativity on the force waveform during twitches.

In the second portion of the study, calcium transients and isovolumic pressure transients were measured from isolated isovolumically contracting rat and ferret hearts. The purpose of these studies was to determine whether the three- or four-state models could be used to predict the pressure waveforms from simultaneously measured calcium transients. Data were collected during normal regularly timed contractions, spontaneously occurring trains of irregularly timed contractions, and the onset of rapid pacing-induced tetanic contractions after ryanodine administration. As described above, the differential equations of the three- and four-state models with and without cooperativity were solved numerically with Newton's method with the measured calcium transients as the driving function and predicted isometric force (or pressure) as the output. The rate constants of the models were adjusted to provide the best possible fit between measured and predicted pressure waves with an algorithm described in detailed below. Because, for isovolumic contractions, instantaneous left ventricular (LV) pressure (LVP) is proportional to instantaneous mean circumferential muscle stress (12, 15) and, in the models, muscle stress is proportional to the number of strong actin-myosin bonds, measured and predicted pressure curves were normalized to a magnitude of 1 to obviate the necessity of dealing with several proportionality constants related simply to fixed values of muscle mass, chamber geometry, and muscle architecture.

The degree of concordance between the model-predicted normalized force [$F_{p,n}(t)$] and the measured normalized force [$F_{m,n}(t)$] curves was quantified by determining the root-mean-squared difference (D_{RMS}) between the two curves

$$D_{RMS} = \frac{1}{T}\{\int[F_{m,n}(t) - F_{p,n}(t)]^2\, dt\}^{1/2} \quad (2)$$

where T is the duration over which the integration is performed. D_{RMS} values obtained with the three- and four-state models with and without cooperativity were compared, and the information was used in assessing superiority of one model over another.

Experimental Procedures

Langendorff preparation. In each experiment, a male Wistar rat (350–450 g body weight) or an 8- to 14-wk-old ferret (1.2- to 1.4-kg body weight) was heparinized (1,000 U ip) and then anesthetized with ketamine (100 mg/kg ip) and xylazine (1 mg ip). A bilateral sternotomy was performed, and the heart was rapidly excised and immediately submerged in oxygenated, warmed, modified Tyrode solution (34°C, composition provided below). The severed end of the aorta was fed over a 16-gauge needle that was connected to a modified Langendorff perfusion system, and perfusate flow was adjusted to provide a perfusion pressure of ~70–80 mmHg. The left atrium was opened. A latex balloon attached to the end of stiff polyethylene tubing, with fenestrations on the distal 2–3 mm of its tip, was inserted into the LV and held in place by a 2-0 silk purse-string suture placed around the mitral annulus. The balloon and tubing were filled with water and connected to a Statham pressure transducer for measurement of LVP. Balloon volume could then be varied with a calibrated 2-ml syringe. Two pacing electrodes were positioned in the right ventricular outflow tract and the right atrium.

The perfusion system consisted of a warmed storage vat for perfusate solutions, an adjustable speed rotary pump (Masterflex), and a Pyrex condenser. The vat and condenser were warmed by a constant-temperature circulator set to heat the solutions to 34°C. The perfusate was composed of (in mmol/l) 15 glucose, 140 NaCl, 5 KCl, 0.9 $MgCl_2$, 2.0 $CaCl_2$, and 6 *N*-2-hydroxyethylpiperazine-*N'*-2-ethanesulfonic acid (HEPES). Ferret hearts were exposed to ryanodine (3 mM for 20–30 min), and the $CaCl_2$ concentration was increased to between 5 and 10 mM to achieve tetanic contractions with high-pressure generation (25, 32). The pH was adjusted to 7.40 and equilibrated with 100% O_2. The perfusate was not recirculated. After attachment of the heart to the modified Langendorff perfusion system, ventricular volume was adjusted to provide an end-diastolic pressure of ~10 mmHg, and the hearts were allowed to stabilize for at least 20 min; the end of the stabilization period was defined as the time when peak LVP and coronary perfusion pressure attained stable levels.

Aequorin macroinjection, signal recording, and calibration of aequorin light signals. Techniques for measuring calcium transients from the epicardial surface of crystalloid-perfused hearts were similar to those described previously (3, 22, 32). An aequorin solution (1 mg/ml of aequorin, 154 mmol/l of NaCl, 5.4 mmol/l of KCl, 1 mmol/l of $MgCl_2$, 12 mmol/l of HEPES, 11 mmol/l of glucose, and 0.1 mmol/l of EDTA, adjusted to pH 7.40) was prepared. After stabilization, 3–5 μl of this solution were injected just under the epimysium in the inferoapical region with a low-resistance glass micropipette with an inner diameter of ~30 μm.

To record the aequorin luminescence, the heart and a portion of the perfusion apparatus was placed inside a lighttight box (Gary Harrar Associates, Rochester, MN) that is identical in design to that originally used for aequorin experiments on papillary muscles (4) and described in detail previously (22). The heart was positioned within a specially designed glass organ bath with a concavity at its base; the inferoapical region of the heart (the aequorin injection site) was placed in contact with this base so that the aequorin luminescence was emitted through the bottom of the bath.

The bottom of the organ bath was, in turn, positioned at the focal point of an ellipsoidal light collector, which directed the light to the surface of a photo multiplier tube (9235QA, Thorn EMI, Fairfield, NJ). The photo multiplier was energized by a power supply (PM28R, Thorn EMI) with the voltage adjusted to provide an optimal signal-to-noise ratio (900 V). The aequorin light signal was recorded as anodal current, with zero set as the mean dark current. Initial filtering was performed on-line with an analog filter with a corner frequency of 100 Hz.

The method of calibrating the light signal into an absolute concentration of intracellular calcium ($[Ca^{2+}]_i$) was the same as that used in papillary muscles and described previously (22). At the end of the experiment, the heart was perfused with a 50 mmol/l calcium-5% Triton X-100 solution that lysed the cells and exposed the remaining aequorin to high amounts of calcium (3). Luminescence signals to be converted to calcium signals (L) were normalized by the total light emission (L_{max}), which was estimated as the integral of the aequorin signal collected during the lysis procedure multiplied by the rate constant for aequorin consumption (2.11/s) (22). The instantaneous L/L_{max} was then converted to time-varying $[Ca^{2+}]_i$ according to the following equation

$$L/L_{max} = [(1 + K_r[Ca^{2+}]_i)/(1 + K_{tr} + K_r[Ca^{2+}]_i)]^3 \quad (3)$$

where K_r (4.5×10^6/M) and K_{tr} (130) are the rate constants for the relationship between light and calcium concentration, respectively (22).

Filtering and signal averaging. Three types of contractions were analyzed in the present study: *1*) normal twitch contractions, *2*) spontaneous arrhythmias occurring during the course of an experiment, and *3*) tetanic contractions induced by rapid pacing at 10 Hz after exposure to ryanodine. For normal twitch contractions, repetitive sequences of steady-state contractions were pooled, and the LVP waves and corresponding aequorin transients were averaged. In this fashion, a composite LVP transient was derived with an average intracellular calcium transient. For arrhythmias and tetanus data, where signal averaging cannot be used because one beat differs from the next, a three-point median filter was employed. The median filter simply replaces a point in a sequence with the median of the sequence of its nearest neighbors, thus functioning as a low-pass filter.

Parameter-fitting algorithm. A predicted ventricular pressure or muscle force curve was generated from the model (three-state or four-state) based on the measured calcium transient and specified parameter values as described in *Theoretical Considerations*. Initial values for the parameters were set equal to those shown previously to be reasonable for cardiac muscle (7). A range of possible values was also specified, over which each parameter was allowed to vary; this range was centered about the default values and was sufficiently broad so that the upper and lower limits were at least one order of magnitude above and below these values, respectively.

To optimize the fit between the measured and predicted pressures, a global nonlinear Nelder-Mead search algorithm was employed. In general terms, this algorithm searches an n-dimensional space for the optimum parameter set that minimizes the root-mean-square error between the experimentally observed and predicted pressure curves (D_{RMS}; *Eq. 2*). After optimization, the 95% confidence interval about the optimal value of each parameter is determined by separately increasing and decreasing the parameter value from its optimal value until the D_{RMS} increases by 5% of its lowest value (31).

RESULTS

Theoretical Analyses

Interrelating muscle force and calcium transient. It has been shown previously (7) that the four-state model with seven rate constants can accurately predict muscle force from a calcium transient measured with aequorin. The first test performed in the present study was to determine whether deletion of the calcium-free, force-generating state (i.e., the fourth state) impacted on the ability to predict force. The results are shown in Fig. 2. Figure 2*A* shows the calcium transient and the simultaneously measured isometric force obtained from the literature (34). Figure 2*B* shows the best fits provided by the three-state and four-state models; no cooperativity was introduced into either model at this point. As shown, both models provide reasonably good fits in this example, but significant differences are present. The main difference between the two models is during relaxation where the four-state model is better able to simulate the curve than the three-state model, which relaxes significantly slower. This difference in fit between the two models is also revealed in the D_{RMS} values, which were lower for the four-state than for the three-state model. Surprisingly, the addition of cooperativity did not improve the three-state prediction and had little impact on the four-state model because the fit to the data was already excellent with that model (see *Impact of cooperativity*).

Time course of bound calcium. The purpose of the next analysis was to compare model predictions of the time course of bound calcium. The rationale for performing this analysis was that the results of previous experimental studies have suggested that calcium bound to the myofilaments returns to resting levels during the early stages of relaxation (34); this observation has contributed importantly to the notion that the calcium-free, force-generating state (i.e., the fourth state in Fig. 1, gray area) is required for explaining the events occurring during twitches in cardiac muscle and that the three-state model could not account for this phenomenon. However, as shown in Fig. 3*A*, in contrast to previous assumptions, the time course of the bound calcium, normalized to its own peak value, is very similar for the three- and four-state models. Both show that bound calcium declines and reaches diastolic levels during midrelaxation. However, the difference between the models is revealed when force and bound calcium are plotted in absolute terms as shown in Fig. 3, *B* and *C*, which indicate significant quantitative differences. First, peak bound-calcium concentration is almost three times greater for the three-state than for the four-state model (Fig. 3*B*). A magnified view of the absolute bound-calcium concentration plotted along with predicted force (also shown in absolute terms) is shown in Fig. 3*C*. These graphs demonstrate that equal force is produced with much less bound calcium in the four-state model, suggesting a greater "calcium efficiency" of contraction. It is also significant in the four-state model that the bound calcium declines slightly below the force curve during late relaxation, indicating

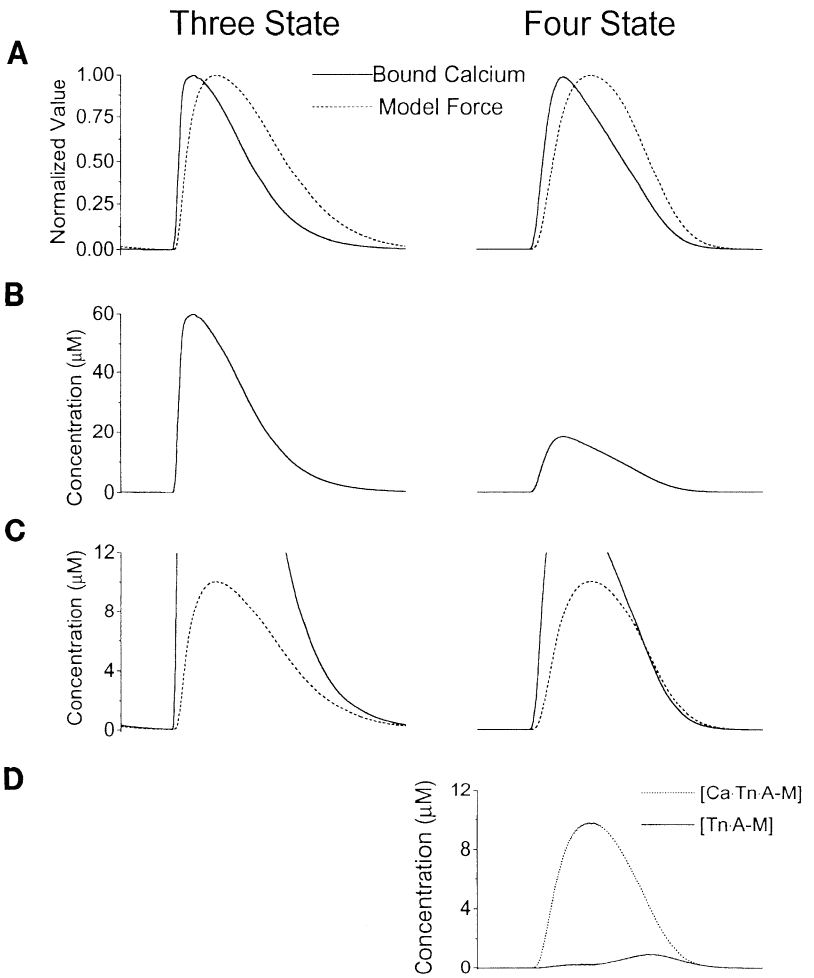

Fig. 3. Examination of time course of bound calcium relative to force transient. *A*: in contrast to previous assumptions, when normalized to their respective amplitudes, both 3- and 4-state models predict that bound calcium decays well in advance of force. *B*: when expressed in absolute terms, it is seen that for comparable force generation, much less calcium is required in 4-state model, suggesting a greater calcium efficiency with that biochemical scheme. *C*: it is apparent that amount of bound calcium can fall below number of force-generating units only in 4-state model. *D*: absolute amount of calcium-free, force-generating units is small compared with total force, suggesting a different physiological role of that state.

that there can be force generation without calcium binding, but this is only a small amount. In contrast, bound calcium never falls below force in the three-state model. Thus because bound calcium declines significantly before force declines in both models, this feature cannot be used to distinguish the two models.

It is further pertinent to determine for the four-state model the relative contribution of the calcium-free strong actin-myosin-bound moiety to total force. The result of this analysis for the representative contraction is illustrated in Fig. 3*D*. As suggested in a previous theoretical study (7), the calcium-free, actin-myosin bond contributes very little to total force production, with a vast majority of force due to strong actin-myosin binding in the presence of calcium. However, the importance of the fourth state is revealed by the fact that the net flux through the dissociation constant for the four-state model (K_d') pathway is more than 2.5-fold greater than flux through the dissociation constant for the three-state model (K_d) pathway; this is because once in the fourth state, there is a great propensity for actin-myosin uncoupling (relaxation). This indicates that one physiological role of the fourth state is to provide for relaxation kinetics, which are independent of contraction kinetics. This contrasts with the three-state model in which relaxation and contraction kinetics are linked through related pathways (K_a and K_d pathways, respectively).

Time course of force recovery after a muscle length impulse. One experimental approach to assessing the time course of bound calcium has been to measure the time course of force recovery after a rapid muscle length impulse (27). With this approach, it is assumed that the length impulse uncouples strong actin-myosin bonds (pushing the system to *states 1* or *2* of Fig. 1) and that the initial rate of rise in force will be proportional to the amount of bound calcium [i.e., calcium bound to tropinin on actin bound to myosin with a weak bond ($[Ca^{2+} \cdot Tn \cdot A \sim M]$)]. This experiment was simulated to test for a fundamental difference in response to a length impulse that could help distinguish the two models. Accordingly, the rapid length impulse was simulated by transferring the contents of *state 3* and *state 4* to *state 2* and *state 1*, respectively (Fig. 1), at the desired moment during the cardiac cycle and then determining the rate of rise in force regeneration (initial dF/dt). The result of this analysis for the four-state model is shown in Fig. 4*A* where the force tracings resulting from a normal contraction and simulated length impulses at various times after the onset of contraction are shown. These tracings bear a striking resemblance to those previously obtained experimentally in isolated cardiac muscle. The initial dF/dt was determined for each curve (with many more time points investigated than shown in Fig. 4) and was then plotted as a function of the time of the length impulse; for

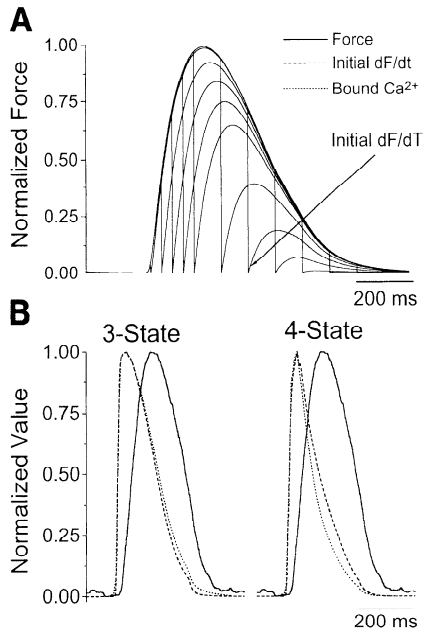

Fig. 4. *A*: examples of predicted force for differently timed simulated muscle length impulses (obtained with 4-state model). Rate of force regeneration (initial dF/d*t*) has been proposed as an index of relative bound calcium (27). *B*: time course of initial dF/d*t* relative to respective model-predicted bound calcium and force for both models. As shown, initial dF/d*t* correlates well with time course of bound calcium but, in contrast to previous assumptions, predicted behavior is similar for both models.

comparison, these curves were superimposed on curves of their respective actual model-calculated bound-calcium and force tracings; all curves were normalized to their respective maximum values as shown in Fig. 4*B*. Although there were subtle quantitative differences, it is evident that both models behaved similarly: the time course of initial dF/d*t* from a length impulse rose rapidly after the onset of contraction, peaked during midcontraction, and declined in advance of relaxation. Furthermore, initial dF/d*t* was closely related to instantaneous bound calcium in both models. Thus the rate of force recovery from length impulses imposed at different times during a contraction cannot be used to distinguish the two models.

Equilibrium vs. twitch force-[Ca^{2+}]$_i$ relationships. The relationship between force and peak intracellular calcium differs significantly among normal twitches, slow twitches, and equilibrium conditions (35). To determine whether these characteristics could distinguish between the two models, normal twitch contractions with different peak [Ca^{2+}]$_i$ values were simulated by scaling the calcium transient of Fig. 2 to have a peak value ranging between 0 and 10 μM. Slowed contractions, which simulate those measured experimentally after exposure of the myocardium to ryanodine, were simulated by expanding the time scale of the calcium transient in Fig. 2 and then varying its amplitude as in the first example. Finally, equilibrium contractions, which simulate tetanii, were simulated by setting [Ca^{2+}]$_i$ to a steady level, which was varied after equilibrium conditions had been achieved. The results, shown in Fig. 5, reveal a major difference between the two models. During each type of contraction, there was a typical sigmoidal relationship between force and [Ca^{2+}]$_i$. For the three-state model, the normal and slowed twitch contractions deviated only slightly from the equilibrium relationship. In contrast, for the four-state model, normal twitches fell markedly below the equilibrium curve and slowed contractions fell between the two extremes. For example, with a [Ca^{2+}]$_i$ value of 1 μM (Fig. 5, vertical line) normal twitch force was slightly less than one-half of that achieved during equilibrium conditions, whereas slowed contractions achieve ~60% of the equilibrium value. A previous experimental study (35) revealed behavior nearly identical to that of the four-state model. Thus these characteristics are major experimentally verifiable distinguishing features between the two models.

Impact of cooperativity. The analyses described in thus far were performed without any specific provisions incorporated to account for myofilament cooperativity. We therefore tested the impact of introducing varying amounts of cooperativity on the relationship between calcium and force generation during twitch contractions. Cooperativity was introduced as summarized in METHODS (*Eq. 1*). Analyses were performed with cooperativity introduced into K_1 (myofilament calcium affinity) and K_a (actin-myosin affinity) separately or with cooperativity introduced into both rate constants simultaneously; results were similar with all three types of analyses, and, therefore, only one will be presented. Of note was the fact that all other parameter values were maintained constant on moving from the simulation of one Hill coefficient to another. Another constraint imposed during this analysis was that the K_{50} values were the same for both the three- and four-state models (0.5 μM). The results obtained with cooperativity simultaneously introduced into both K_1 and K_a are summarized in Fig. 6. The resulting equilibrium force-[Ca^{2+}]$_i$ curves, shown in Fig. 6*A* for the three- and four-state models, reveal that we were successful in modifying the steepness of the curves (Hill coefficients of 2, 4, and 6) while maintaining the K_{50} essentially constant. One property

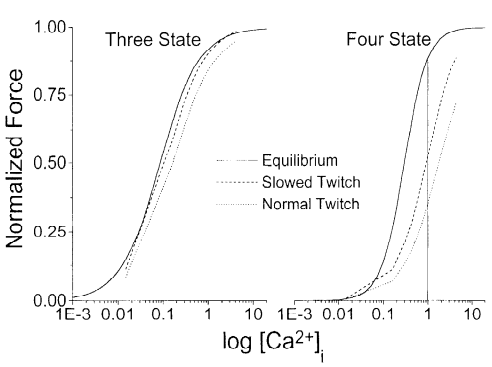

Fig. 5. Force-intracellular Ca^{2+} concentration ([Ca^{2+}]$_i$) relationships predicted by 3- and 4-state models for different types of contractions: normal twitches, slowed twitches (as would be observed after ryanodine exposure), and during equilibrium conditions (as would be observed during tetanic contractions). As shown, there is a big difference between 3- and 4-state model predictions, with only 4-state model exhibiting characteristics similar to those measured in isolated cardiac muscle. See text for details.

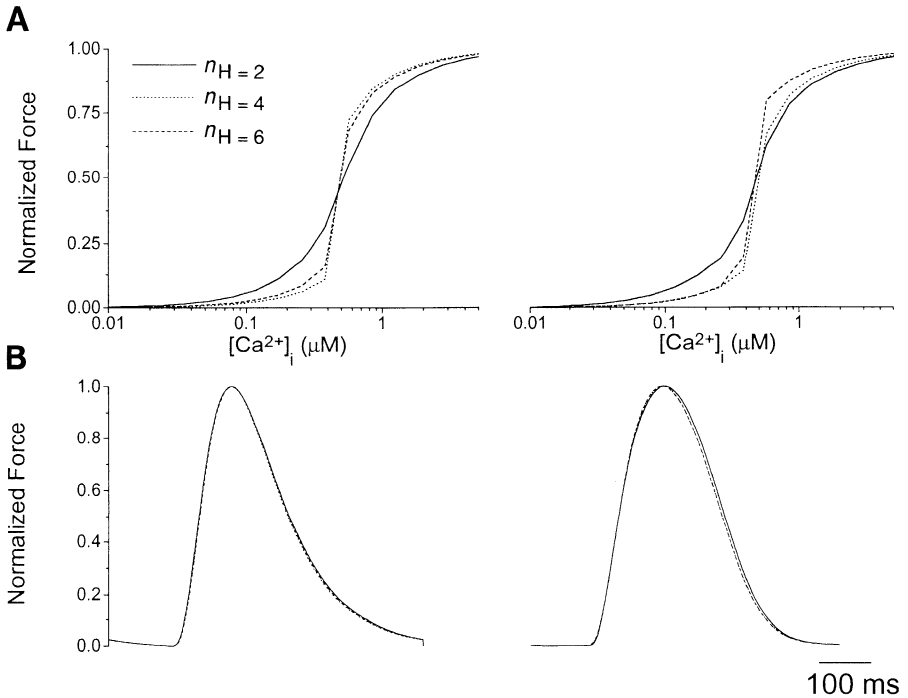

Fig. 6. Impact of cooperativity on model predictions. *A*: equilibrium force-$[Ca^{2+}]_i$ relationships with different degrees of cooperativity incorporated into model; these demonstrate that we were successful in manipulating parameter values (*Eq. 1*) to achieve increasingly higher Hill coefficients (n_H) while maintaining $[Ca^{2+}]_i$ for half-maximal activation constant. Despite these marked changes in equilibrium curves, shape of twitch force transient (*B*) was little affected in either model, a theme that was consistent over a wide range of calcium transients and parameter values.

of both models is that with cooperativity incorporated in this manner, the force-$[Ca^{2+}]_i$ curves are asymmetric around the K_{50} point (steeper at low than at high $[Ca^{2+}]_i$ values), a feature that has been noted in a previous experimental study (19). The effect of varying degrees of cooperativity on the force transient (all with the same calcium transient of Fig. 2) is shown in Fig. 6*B*. Surprisingly, cooperativity had very little effect on the time course of force predicted from the common calcium transient. There were, however, slight differences in absolute peak force generation, which decreased as the Hill coefficient increased (data not shown).

Force-calcium relationships during twitches when calcium is measured with fura 2. Calcium transients measured with fura 2 and other fluorescent indicators differ from those measured with aequorin primarily in that the estimated free-calcium concentration decays much more slowly during diastole. Whereas fura 2 has a higher calcium binding affinity and is a more sensitive calcium indicator than aequorin at diastolic calcium concentrations, there is no general agreement as to which of these types of indicators provides the most accurate estimate of free-calcium concentration. To determine whether such differences impact on the ability of the three- and four-state models to interrelate calcium and force, we analyzed a representative fura 2 calcium transient. As for the aequorin analysis, a fura 2-derived calcium transient was obtained by digitizing previously published data (2); this example is typical in that the calcium concentration remains elevated and decays slowly during diastole. As illustrated in Fig. 7, the results of the analysis differed from those obtained with the aequorin transients in three important respects. First, in the absence of cooperativity, neither the three- nor four-state models provided good fits to the data. Second, the addition of cooperativity into the model had a big impact on the shape of the predicted force transient, although there was still a big difference between the three- and four-state models. Third, only the four-state model with cooperativity provided a good fit to the data. Quantitative results summarized in Table 1 revealed that not only did the four-state cooperative model provide the lowest D_{RMS} value but also was the only model to provide physiological values for K_{50} and the Hill coefficient.

Thus the analyses performed in *Interrelating muscle force and calcium transient* indicated that both the three- and four-state models can account for the relationship between calcium and force on normal twitches when calcium decays quickly during diastole as suggested by aequorin transients. In contrast, in the case where calcium remains elevated and decays more slowly during diastole (as with the fura 2 signal), only the four-state model with cooperativity is adequate to interrelate force and calcium on a normal steady-state twitch. With regard to equilibrium force-calcium relationships, which have not been noted to differ between aequorin and fura 2 measurements, only the four-state model with cooperativity could account for all of the phenomena examined.

Experimental Findings

Steady-state beats. LVP waves and aequorin luminescence transients were recorded during normal twitch contractions from 12 isolated isovolumically contracting rat hearts. The signal-to-noise ratio was decreased by signal averaging between 15 and 20 beats. Next, the three- and four-state noncooperative models were applied. A typical example is shown in Fig. 8. Both models provided reasonable fits to the experimentally observed data, with the chief differences noted during relaxation

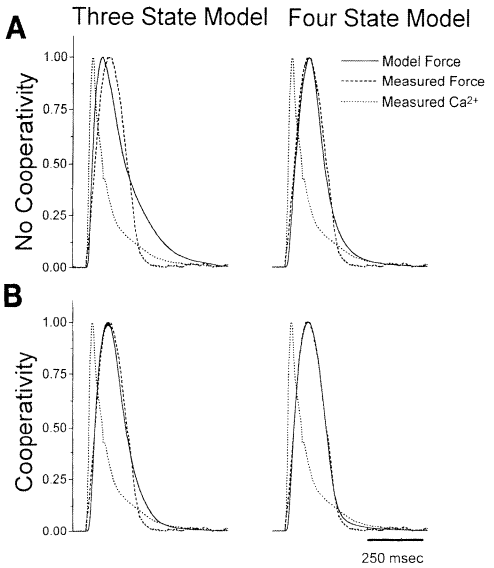

Fig. 7. Force and calcium transients estimated by fura 2 method obtained from literature (2) for 3- and 4-state model without (*A*) and with (*B*) cooperativity were digitized and subjected to analysis. As shown, calcium transient decays more slowly during diastole and retains a substantial value throughout late part of beat. Important finding was that only 4-state model with cooperativity could provide a reasonable prediction of measured force from calcium transient. See text for more details.

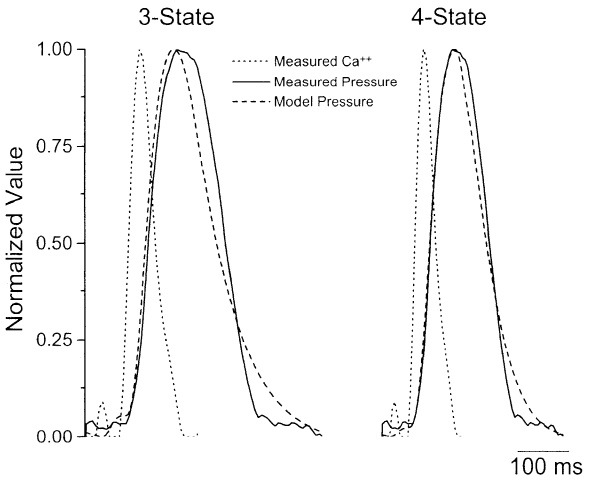

Fig. 8. Representative signal-averaged measured calcium transient and pressure wave from Langendorff-perfused rat heart. Similar to isolated muscle (see Fig. 2), 4-state model overall provides only a slightly better prediction of pressure than 3-state model; major difference is seen during late relaxation where 4-state model is significantly better. See text for additional details.

where the four-state model provided a significantly better fit. Twitch contractions examined from other hearts were similar. The addition of cooperativity did not significantly affect the closeness of the fits, consistent with the findings above (Fig. 6). Mean (±SD) parameter values required to achieve best fits with the different models are also summarized in Table 2. As shown, the standard deviations are relatively large compared with the mean values for several of the parameters. This is due to the high degree of interdependence among the parameter values. To provide a quantitative index of the comparison of the different models, D_{RMS} was determined with optimal parameter values. As summarized in Table 2, there was little difference in D_{RMS} values among the various models; thus despite the consistent finding that the three-state model did not fit the late portion of relaxation, D_{RMS} values were not sensitive to this.

Arrhythmias. Spontaneous arrhythmias were chosen from segments of recorded tracings in the rat hearts. The aequorin tracing was converted into a calcium transient and then median filtered (unlike normal twitch contractions, signal averaging could not be used because each beat differed from the next). Contraction sequences were analyzed with the parameter search routine to optimize the fit between the experimentally observed and the model-predicted pressure transients. Representative results, obtained with cooperativity included in both models, are shown in Fig. 9. The low-pass filtered calcium transient during arrhythmia is shown in Fig. 9*A*. Similar to the findings obtained with steady-state contractions, the three- and four-state models provided similar fits to the measured pressure waveforms, with the four-state model providing better fits during late relaxation. Furthermore, the inclusion of cooperativity did not significantly affect the shape of the pressure waveform (consistent with find-

Table 1. *D_{RMS}, K_{50}, and Hill coefficient values from best-fit rate constants to a steady-state force curve*

Model	D_{RMS}	K_{50}, μM	n_H
3 State			
Without cooperativity	4.48	310	1.5
With cooperativity	1.91	0.47	20
4 State			
Without cooperativity	1.96	0.78	1.7
With cooperativity	0.95	0.24	3.1

Values were derived with calcium measured with fura 2 (2). D_{RMS}, root-mean-squared difference; K_{50}, half-maximal activation; n_H, Hill coefficient.

Table 2. *Best-fit parameter values for different models obtained when fitting steady-state isovolumic contractions in isolated rat hearts*

	3 State		4 State	
Parameter	Without	With	Without	With
K_1, $(\mu M \cdot s)^{-1}$	218±156		1.2±0.3	
α_1, $(\mu M \cdot s)^{-1}$		7.5±10		5.0±2.8
β_1, $(\mu M \cdot s)^{-1}$		11±8		10±5
K_2, s^{-1}			16,827±13,130	11,380±7,531
K_3, s^{-1}	54±22	608±78	121±80	84±33
K_4, s^{-1}			53±20	52±17
K_a, $(\mu M \cdot s^{-1})$	0.06±0.02		0.43±.53	
α_a, $(\mu M \cdot s)^{-1}$		0.30±0.43		0.25±0.43
β_a, $(\mu M \cdot s)^{-1}$		0.18±0.23		$2.9 \pm 8.4 \cdot 10^{-5}$
K_d, s^{-1}	21±17	8.4±3.5		5.3±4.8
K'_d s^{-1}			19.4±14.2	14.6±7.3
D_{RMS}	6.1±3.6	7.3±3.5	4.8±3.3	5.6±3.9

Values are means ± SD. Without, without cooperativity; with, with cooperativity; K_1, K_2, K_3, and K_4, calcium-binding affinities (rate constants) for *states 1–4*, respectively; α and β, adjustable constants; K_a, association constant (actin-myosin affinity); K_d and K'_d, dissociation constant for 3-state and 4-state models, respectively; RMS, root-mean-square error.

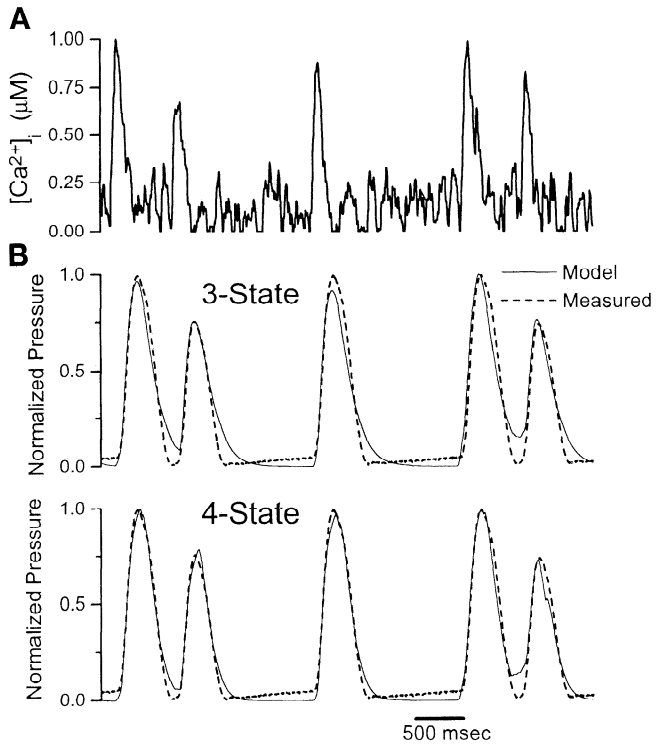

Fig. 9. Representative calcium transients (*A*) and pressure waves (*B*) measured from Langendorff rat heart during spontaneous arrhythmias. Note that increased noise in calcium transient compared with previous example is because these transients cannot be signal averaged. As seen in *B*, similar to normal contractions, 3- and 4-state model fits were comparable, again with differences noted predominantly during late relaxation.

ings reported above). Accordingly, D_{RMS} values obtained for these complex contraction sequences did not vary significantly among the different models, as shown in Table 3. Best values for rate-constant values of the various models are also summarized in Table 3. Four additional examples, shown in Fig. 10, show the relatively good fit afforded by the four-state cooperative model during complex arrhythmic contraction sequences. It is noteworthy that the fits to the data are as good as they are considering the fact that the calcium transients are obtained from filtered (and not signal-averaged) macroinjected aequorin luminescence.

Table 3. *Best-fit parameter values for different models obtained when fitting spontaneous arrhythmias during isovolumic contractions in isolated rat hearts*

	3 State		4 State	
Parameter	Without	With	Without	With
K_1, $(\mu M \cdot s)^{-1}$	1.0 ± 0.1		2.2 ± 0.9	
α_1, $(\mu M \cdot s)^{-1}$		5.8 ± 3.4		3.0 ± 4.7
β_1, $(\mu M \cdot s)^{-1}$		7.1 ± 5.7		9.1 ± 5.4
K_2, s^{-1}			12,145 ± 9,827	4,994 ± 4,655
K_3, s^{-1}	26 ± 11	513 ± 80	30 ± 13	25 ± 9
K_4, s^{-1}			41 ± 27	64 ± 57
K_a, $(\mu M \cdot s^{-1})$	0.10 ± 0.01		0.12 ± 0.03	
α_a, $(\mu M \cdot s)^{-1}$		0.18 ± 0.23		0.005 ± 0.003
β_a, $(\mu M \cdot s)^{-1}$		0.77 ± 0.94		0.002 ± 0.004
K_d, s^{-1}	26 ± 11	13 ± 8	11 ± 13	17 ± 19
K'_d, s^{-1}			32 ± 16	33 ± 17
D_{RMS}	1.33 ± 0.27	1.89 ± 0.33	1.25 ± .26	1.21 ± 0.25

Values are means ± SD.

Onset of tetanic contracture. Next, consideration was given to the unique, complex pressure and calcium waveforms observed during the induction of tetanus in intact ferret hearts. The pressure waveform during rapid (10 Hz) pacing after exposure to ryanodine features a steady rise in pressure, culminating in a plateau with oscillations. Figure 11 shows a representative example. Figure 11*A* shows the median filtered calcium transient. Figure 11*B* shows the normalized measured pressure and the predicted force based on the indicated model configuration. The four-state model with cooperativity provides an excellent prediction of the force curve during the preceding steady-state beats, the ascent in pressure, and the plateau where there were significant pressure oscillations. Note that, in contrast to the results obtained with normal and arrhythmic contractions, there was a substantial difference between the models and that the inclusion of cooperativity significantly affected the pressure waveform. For these contractions, there was a clear difference between the models, with the four-state cooperative model providing a significantly better fit to the data. Quantitative results (D_{RMS} values summarized in Table 4) substantiate this observation by showing that the D_{RMS} values obtained with the four-state models were significantly better than those obtained with the three-state models. Results from an additional four examples, shown in Fig. 12, confirm the ability of the four-state cooperative model to predict these complex pressure waveforms from the measured calcium transients. The parameter values required to achieve the best fits are also summarized in Table 4. As for the other types of contractions, the parameter values differed significantly among the different models and standard deviations about the means were relatively large, as noted above, because of the interdependence among the parameter values.

To explore the physiological meaning of the different parameter values, we calculated the K_{50} values and Hill coefficients resulting from the best-fit rate constants for each of the models. The results are summarized in Table 5. It is interesting to note that the values of these two parameters obtained for the four-state cooperative model (~0.4 μM and ~4, respectively) are similar to those measured previously in these ferret hearts (32). In contrast, values of these parameters obtained for the other models differed significantly from those obtained with the four-state cooperative model.

DISCUSSION

In an attempt to evolve from phenomenological descriptions (28–30), investigators (7, 9, 17, 23) have turned toward more mechanistic theories of cardiac muscle contraction to explain ventricular pump properties. Whereas previous efforts in this regard (7, 9, 17, 23) have been limited to theoretical analyses, the present effort represents an initial attempt to quantitatively bridge theoretical and experimental aspects of this fundamental problem. The strategy of the present

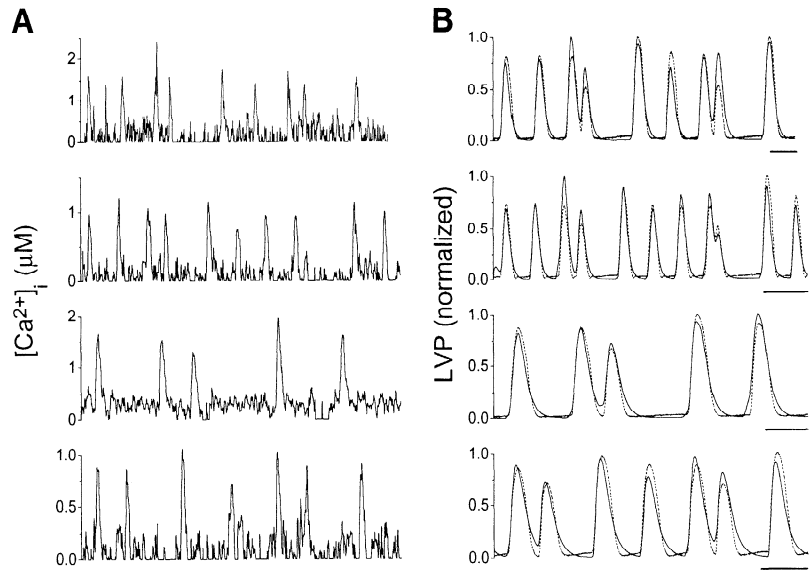

Fig. 10. Four additional representative examples of arrhythmias from different hearts showing measured $[Ca^{2+}]_i$ transient (*A*) and measured and best-fit 4-state model prediction [left ventricular pressure (LVP); *B*]. These show that model can provide excellent predictions, even during very complex contraction sequences despite fact that calcium transients were non-signal-averaged signals provided by macroinjected aequorin.

study was to critically evaluate and compare a wide range of characteristics of competing theories with varying degrees of complexity (Fig. 1) on both theoretical and experimental grounds. It is shown that only the four-state cooperative model was able to explain all of the aspects of cardiac physiology explored. This conclusion differs from a similar analysis of skeletal muscle physiology, which provided evidence that the three-state model is sufficient to explain the interrelationships between free-calcium transients and force production under a wide range of conditions (31). Although several of the analyses failed to show superiority of the four-state model based on D_{RMS} values during normal and arrhythmic twitch contractions (Tables 2 and 3), it was evident in every case that the four-state model always provided a significantly better fit during the diastolic portion of pressure and force tracings; D_{RMS}, which examines the entire beat, was an insensitive measure of this specific phase of the contraction.

Although several earlier studies advocated the necessity of the four-state model in explaining cardiac physiology (27, 34), two of the primary attributes assigned to the fourth state, which had been assumed to render it required over the three-state model, were not substantiated by the present analysis. The first relates to the

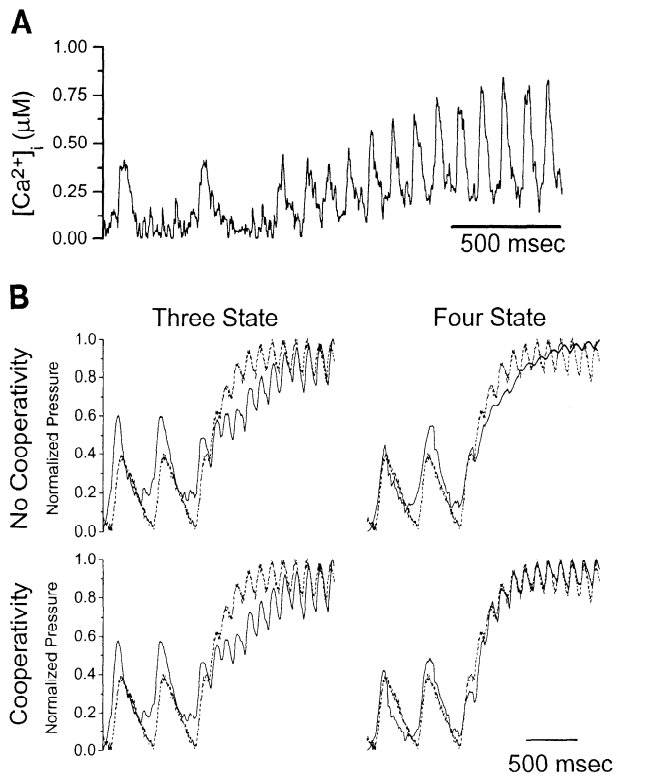

Fig. 11. Representative example of $[Ca^{2+}]_i$ measured during onset of rapid pacing to induce a tetanic contraction (*A*) and simultaneously measured pressure curves (*B*) along with prediction of each of 4 models (3- and 4-state models without and with cooperativity). Dashed lines, normalized measured pressure; solid lines, best fit model-predicted pressure. In contrast to twitch contractions, these complex pressure tracings were much better fit by 4-state cooperative model, with which fine details of pressure wave could be accounted for. In addition, that model was able to simultaneously account for twitch contractions on normal beats preceding onset of rapid pacing.

Table 4. *Best-fit parameter values for different models obtained when fitting onset of rapid pacing-induced tetanic contractions in isovolumically contracting isolated ferret hearts*

	3 State		4 State	
Parameter	Without	With	Without	With
K_1, $(\mu M \cdot s)^{-1}$	262±113		23±19	
α_1, $(\mu M \cdot s)^{-1}$		41±36		0.68±0.25
β_1, $(\mu M \cdot s)^{-1}$		4.4±5.4		10.0±3.7
K_2, s^{-1}			8,592±5,773	13,232±11,196
K_3, s^{-1}	550±137	37±29	45±41	183±144
K_4, s^{-1}			148±18	134±79
K_a, $(\mu M \cdot s^{-1})$	0.05±0.01		0.23±0.01	
α_a, $(\mu M \cdot s)^{-1}$		0±0.001		0.24±0.27
β_a, $(\mu M \cdot s)^{-1}$		0.06±0.07		1.20±1.40
K_d, s^{-1}	22±4	33±14	0.04±0.08	8.3±7.3
K'_d, s^{-1}			84±36	91±39
D_{RMS}	4.69±0.89	4.35±0.91	3.41±0.58*	2.28±0.89*

Values are means ± SD. *$P < 0.05$ compared with other RMS values by analysis of variance with Tukey's post hoc test.

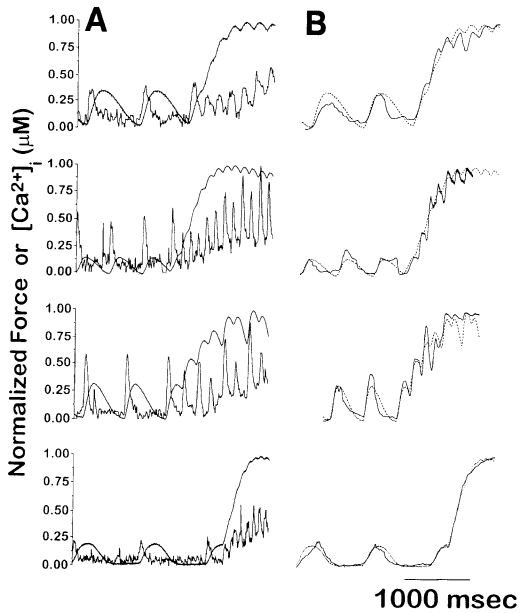

Fig. 12. *A*: additional examples (each from a different heart) showing measured $[Ca^{2+}]_i$ and force transients at onset of rapid pacing. *B*: best-fit 4-state cooperative model curves (solid lines) consistently provides a good fit to measured pressure curves (dashed lines) during these complex and varied contraction patterns.

fact that when measured with aequorin, intracellular free-calcium concentration falls to diastolic levels before force returns to diastolic levels (as in Fig. 2) (33, 34). Accordingly, it was hypothesized previously that there must be a substantial amount of calcium-free force-generating units during the latter half of contraction. However, several aspects of the present analysis suggest that peak [Tn·A-M] values are small compared with the total number of strong bonds formed during a contraction (Fig. 3*D*). Thus instead of making a significant contribution to force production, the results of the present study suggest that one important role of the fourth state in the model is to allow contraction kinetics (rate of cross-bridge formation) to be described predominantly by one set of rate constants (K_1, K_3, K_a, and K_d) and relaxation kinetics (rate of cross-bridge uncoupling) to be described primarily by a separate set of constants (K_2, K_4, and K'_d). This assertion is based on the fact that although peak instantaneous concentrations of [Tn·A-M] are low, the net flux through the K'_d pathway is far greater than the flux through the K_d pathway when optimal rate-constant values are used. The underlying reason may relate to a much greater actin-myosin uncoupling probability in the absence of bound calcium than in the presence of bound calcium (6, 13). This is the reason why, in particular, on a theoretical level, the four-state model was able to explain relaxation kinetics much better than the three-state model.

Table 5. *K_{50}, and Hill coefficient values from best-fit rate constants to tetanii data*

Model	K_{50}, μM	n_H
3 State		
Without cooperativity	1.30 ± 0.37	1.38 ± 0.11
With cooperativity	1.06 ± 0.62	1.14 ± 0.40
4 State		
Without cooperativity	0.88 ± 0.62	1.30 ± 0.51
With cooperativity	0.39 ± 0.82	4.18 ± 1.03

Values are means ± SD.

Furthermore, our analysis of a previously obtained fura 2-derived measurement of intracellular free-calcium concentrations (2) provided an unexpected result. We and others (7, 27) have assumed that with such transients, which exhibit a more slowly decaying calcium transient during diastole, force production would more closely track calcium so that there would be less necessity for the calcium-free, force-generating (fourth) state. In contrast, however, this type of transient was much more heavily reliant on the inclusion of both the fourth state and cooperativity to be able to interrelate instantaneous calcium and force. This was because, in the three-state model, the relatively high-calcium concentrations estimated during relaxation with fura 2 predict much higher forces than are actually measured. As noted above for the aequorin transients, the fourth state improves the situation, not predominantly by contributing substantially to force production but by allowing quicker cross-bridge uncoupling during relaxation. However, for the fura 2 example, it was the combination of the fourth state plus cooperativity that made a good prediction of force possible. With cooperativity, the declining force during relaxation with its concomitant decrease in myofilament calcium sensitivity allowed force to fall at the experimentally observed rate.

The second attribute of the four-state model, which was assumed to differ significantly from the three-state model, relates to the time course of bound calcium. It has been assumed that although the four-state model predicts that bound calcium will fall significantly quicker than force, the three-state model would predict a bound-calcium time course that more closely tracks force. This was also shown not to be the case because when expressed in relative terms [as in a previous experimental study (27)], both models predicted similar behavior (Fig. 3). Although substantial differences between the absolute amounts of bound calcium are predicted between the three- and four-state models (Figs. 3, *B* and *C*), lack of techniques to make such quantitative measurements prevent this from being an experimentally testable differentiating feature at the present time.

To probe the time course of bound calcium, investigators (27) have used indirect techniques such as initial dF/dt from variously timed rapid length impulses. The present analysis suggested that there was a very close association between bound calcium and initial dF/dt predicted by both models and that the time course of initial dF/dt, when expressed in normalized terms, was also similar between the two models. Thus these features, also previously assumed to differ between the two models, could not be employed as a differentiating feature.

Thus in view of the facts that *1*) neither of the two previously assumed major advantages of the four-state model over the three-state model appeared to differentiate the models, *2*) both models provided excellent fits to various types of twitch contractions with aequorin-estimated calcium transients, and *3*) previous findings (31) showed the three-state model to be sufficient in skeletal muscle, it became ever more pertinent to explore as broad a range of physiological characteristics as possible to compare the two models.

Several major experimentally verifiable differentiating characteristics between the models were identified. The first of these was identified in the theoretical portion of the study in which peak force-$[Ca^{2+}]_i$ relationships were explored (Fig. 5). It has been shown experimentally that for a given peak $[Ca^{2+}]_i$, force on a normal twitch is significantly less than force during a tetanic contraction and that force on a slowed contraction (achieved by ryanodine exposure) falls between these two extremes (35). The difference between these various contractions is the degree to which equilibrium conditions are approached; tetanic contractions theoretically reach equilibrium and normal twitches are far from equilibrium, whereas slowed contractions fall in between. The four-state model behavior closely paralleled experimental findings, whereas the three-state model predicted very little difference in force production between the three types of contractions.

A second differentiating feature was revealed in the analysis of tetanic contractions, which also revealed the importance of cooperativity. Because tetanic contractions more closely approximate equilibrium conditions, it is not surprising that cooperativity was important in describing these types of contractions. Even without cooperativity, the four-state model provided a better fit to tetanic contractions, although none of the fine details of the pressure waveform were reproduced in that case (Fig. 11). Just as for the fura 2 example of a normal twitch contraction, cooperativity did not substantially improve the three-state predictions, whereas the four-state cooperative model was able to account for tremendous details of the pressure waveform. As illustrated particularly in the example of Fig. 11, rapid cardiac pacing after exposure to ryanodine caused discrete calcium transients that were of large magnitude and easily detected by the macroinjected aequorin. Along with these calcium releases were synchronized oscillations in the pressure wave, as noted previously during rapid stimulation of isolated cardiac muscles exposed to ryanodine (35). It was remarkable that the four-state model with cooperativity could fairly accurately fit these oscillations not only during the plateau of the tetanii but also during the rising phase of pressure immediately after the initiation of rapid pacing. Furthermore, the four-state cooperative model was able to fit these details of the pressure wave during the tetanii and simultaneously provide a good fit to the preceding steady-state contractions, a feature that was not possible for any of the other models.

Limitations. There are several potential limitations of the present study that should be considered. The experimental aspects of this study focused on measurements made in intact hearts, not in a simpler system such as isolated muscles. However, there are two principal reasons that justify this choice. First, there is increasing evidence, particularly under isovolumic conditions, that the complex geometry, architecture, and activation sequence of the intact heart do not distort the global expression of muscle properties (8, 32). There is also evidence that there is relatively little inhomogeneity in muscle contractile properties throughout the myocardium (8). Thus it can generally be concluded that isovolumic pressure waves are simply scaled versions of the isometric force waves experienced by the average muscle (8). On the other hand, it must be acknowledged that small regional differences in the calcium transient have been identified from apex to base (24), so there is a possibility that the calcium transients measured from the inferoapical epicardium, as in the present study, may not be representative of the true "average" calcium transient in all muscles throughout the LV. Second, as noted above, significant efforts are underway to explain whole heart function under physiological and pathophysiological conditions in terms of basic theories of cardiac muscle contraction. By performing studies in intact hearts, the results of the present study represent another step toward this ultimate goal.

Another potential limitation relates to the fact that our studies rely on macroinjected aequorin to estimate calcium transients. It is well recognized that free-calcium transients measured with aequorin and fluorescent indicators differ as detailed above, particularly during relaxation. However, it has not been generally resolved which of the two types of indicators provide the more accurate assessment of intracellular calcium. We have focused our attention on the aequorin transients because our experimental work has moved toward measuring calcium transients under more intact, physiological conditions such as blood-perfused canine hearts. We have found that macroinjected aequorin can be used in these settings. Although fluorescent indicators have been used in small-crystalloid-perfused hearts (24), it remains to be tested whether they could be used in blood-perfused hearts of larger animals. Nevertheless, it was appropriate to question how the fura 2-derived transients behave in the biochemical models we explored. As detailed above, although there were some differences in the behavior of the models with this type of transient, the ultimate conclusions were the same.

In summary, taken as a whole, the results of the theoretical and experimental aspects of this study provide considerable support for the notion that only the four-state cooperative model can appropriately account for the very wide range of physiological phenomena observed in cardiac muscle and the intact heart. Although the three-state model can be used to simply predict the pressure or force curves from the calcium transient measured with aequorin during normal twitch contractions, this is at the expense of failing to be able to explain the diastolic portion of the curves, to simulta-

neously account for several fundamental features of cardiac muscle physiology, and to arrive at equilibrium constants that differ significantly from physiologically meaningful values (Table 5).

Despite the unambiguous nature and breadth of concepts explored in the present theoretical and experimental analyses, the results of this study are primarily based on quantitative analyses. Although many of the conclusions have already been verified experimentally, several key predictions await such verification; these are primarily predictions related to absolute quantities of bound calcium and to absolute quantities of calcium-free, force-generating units in various conditions. Thus it cannot be fully determined whether the conclusions of the present analysis reflect a fundamental validity of the four-state model or whether they simply reflect the fact that, on a mathematical level, a model as complex and with as many degrees of freedom as the four-state cooperative model is required to explain the plethora of phenomena that are observed in cardiac muscle. This dilemma highlights the importance of developing techniques to make the pertinent experimental measurements. The next frontier to be explored along the lines of this investigation relates to assessing the ability of the four-state theory to account for cardiac performance under physiological loading conditions. When ventricular volume (or muscle length) varies, as during normal ejecting contractions, there are instantaneous length-dependent alterations in apparent calcium binding affinity and alterations in physical factors that impact on pressure (force) generation (18, 21, 26, 32). These factors will need to be incorporated into the theory, as suggested previously (7), and tested experimentally. Thus in addition to the experimental challenges revealed by the present study, many additional steps are needed in the continuing quest for a mechanistic theory of ventricular function.

APPENDIX

The simultaneous differential equations describing each of the three models investigated in the present study are summarized in the following state equations.

Three-State Model

$$d[Tn\cdot A]/dt = -K_1[Ca^{2+}][Tn\cdot A] + K_3[Ca^{2+}\cdot Tn\cdot A]$$

$$d[M]/dt = -K_a[Ca^{2+}\cdot Tn\cdot A][M] + K_d[Ca^{2+}\cdot Tn\cdot A\text{-}M]$$

$$d[Ca^{2+}\cdot Tn\cdot A]/dt = K_1[Ca^{2+}][Tn\cdot A] - K_a[Ca^{2+}\cdot Tn\cdot A][M] - K_3[Ca^{2+}\cdot Tn\cdot A] + K_d[Ca^{2+}\cdot Tn\cdot A\text{-}M]$$

$$d[Ca^{2+}\cdot Tn\cdot A\text{-}M]/dt - K_a[Ca^{2+}\cdot Tn\cdot A][M] - K_d[Ca^{2+}\cdot Tn\cdot A\text{-}M]$$

Four-State Model

$$d[Tn\cdot A]/dt = -K_1[Ca^{2+}][Tn\cdot A] + K_3[Ca\cdot Tn\cdot A] + K'_d[Tn\cdot A\text{-}M]$$

$$d[M]/dt = -K_a[Ca^{2+}\cdot Tn\cdot A][M] + K_d[Ca^{2+}\cdot Tn\cdot A\text{-}M] + K'_d[Tn\cdot A\text{-}M]$$

$$d[Ca^{2+}\cdot Tn\cdot A]/dt = K_1[Ca^{2+}][Tn\cdot A] - (K_a[M] - K_3)[Ca^{2+}\cdot Tn\cdot A] + K_d[Ca\cdot Tn\cdot A\text{-}M]$$

$$d[Ca^{2+}\cdot Tn\cdot A\text{-}M]/dt = K_a[Ca^{2+}\cdot Tn\cdot A][M] - K_d[Ca^{2+}\cdot Tn\cdot A\text{-}M] + K_2[Tn\cdot A\text{-}M]$$

$$d[Tn\cdot A\text{-}M] = K_4[Ca^{2+}\cdot Tn\cdot A\text{-}M] - (K_2 + K'_d)[Tn\cdot A\text{-}M]$$

This work was supported by National Heart, Lung, and Blood Institute Grant R29-HL-51885 and grants from the Whitaker Foundation and the American Heart Association, New York City Affiliate.

Address for reprint requests: D. Burkhoff, Dept. of Medicine, Columbia Univ., 630 W. 168th St., New York, NY 10032.

Received 27 November 1996; accepted in final form 27 March 1997.

REFERENCES

1. **Backx, P. H., W. D. Gao, M. D. Azan-Backx, and E. Marban.** The relationship between contractile force and intracellular [Ca^{2+}] in intact rat cardiac trabeculae. *J. Gen. Physiol.* 105: 1–19, 1995.
2. **Backx, P. H., and H. E. D. J. ter Keurs.** Fluorescent properties of rat cardiac trabeculae microinjected with fura-2 salt. *Am. J. Physiol.* 264 (*Heart Circ. Physiol.* 33): H1098–H1110, 1993.
3. **Bentivegna, L. A., L. W. Ablin, Y. Kihara, and J. P. Morgan.** Altered calcium handling in left ventricular pressure-overload hypertrophy as detected with aequorin in the isolated, perfused ferret hearts. *Circ. Res.* 69: 1538–1545, 1991.
4. **Blinks, J. R.** The use of photoproteins as calcium indicators in cellular physiology, part III. In: *Techniques in Cellular Physiology,* edited by P. F. Baker. Shannon, Ireland: Elsevier/North-Holland Scientific, 1982, p. 1–38.
5. **Brandt, P. W., R. N. Cox, M. Kawai, and T. Robinson.** Regulation of tension in skinned muscle fibers. *J. Gen. Physiol.* 79: 997–1016, 1992.
6. **Bremel, R. D., and A. Weber.** Cooperation within actin filaments in vertebrate muscle. *Nature* 238: 97–101, 1972.
7. **Burkhoff, D.** Explaining load dependence of ventricular contractile properties with a model of excitation-contraction coupling. *J. Mol. Cell. Cardiol.* 26: 959–978, 1994.
8. **Burkhoff, D., and W. C. Hunter.** Applicability of myocardial interval-force relationships to the whole ventricle: studies in isolated perfused hearts. In: *The Interval-Force Relationship of the Heart,* edited by M. I. M. Noble and W. A. Seed. Cambridge, UK: Cambridge University Press, 1992, p. 283–299.
9. **Dobrunz, L. E., P. H. Backx, and D. T. Yue.** Steady-state Ca_i^{2+}-force relationship in intact twitching cardiac muscle: direct evidence for modulation by isoproterenol and EMD 53998. *Biophys. J.* 69: 189–201, 1995.
11. **Gao, W. D., P. H. Backx, M. Azan-Backx, and E. Marban.** Myofilament Ca^{2+} sensitivity in intact versus skinned rat ventricular muscle. *Circ. Res.* 74: 408–415, 1994.
12. **Grossman, W., E. Braunwald, T. Mann, L. P. McLaurin, and L. H. Green.** Contractile state of the left ventricle in man as evaluated from end-systolic pressure-volume relations. *Circulation* 56: 845–852, 1977.
13. **Hill, T.** Two elementary models for the regulation of skeletal muscle contraction by calcium. *Biophys. J.* 44: 383–396, 1983.
14. **Hofmann, P. A., and F. Fuchs.** Evidence for a force-dependent component of calcium binding to cardiac troponin C. *Am. J. Physiol.* 253 (*Cell Physiol.* 22): C541–C546, 1987.
15. **Hunter, W. C., and J. Baan.** The role of wall thickness in the relation between sarcomere dynamics and ventricular dynamics. In: *Cardiac Dynamics,* edited by J. Baan, A. C. Arntzenius, and E. L. Yellin. The Hague: Nijhoff, 1980, p. 123–134.
16. **Huxley, A. F.** Muscle structure and theories of contraction. *Circulation* 1: 255–318, 1958.
17. **Izakov, V. Y., L. B. Katsnelson, F. A. Blyakhman, V. S. Markhasin, and T. F. Shklyar.** Cooperative effects due to calcium binding by troponin and their consequences for contraction and relaxation of cardiac muscle under various conditions of mechanical loading. *Circ. Res.* 69: 1171–1184, 1991.

18. **Jewell, B. R.** A reexamination of the influence of muscle length on myocardial performance. *Circ. Res.* 40: 221–230, 1977.
19. **Julian, F. J., M. R. Sollins, and R. L. Moss.** Absence of a plateau in length-tension relationship of rabbit papillary muscle when internal shortening is prevented. *Nature* 260: 340–342, 1976.
20. **Katsnelson, L. B., V. Y. Izakov, and V. S. Markhasin.** Heart muscle: mathematical modelling of the mechanical activity and modelling of mechanochemical uncoupling. *Gen. Physiol. Biophys.* 9: 219–244, 1990.
21. **Kentish, J. C., H. E. D. J. ter Keurs, L. Ricciardi, J. J. J. Bucx, and M. I. M. Noble.** Comparison between sarcomere length-force relations of intact and skinned trabeculae from rat right ventricle: influence of calcium concentrations on these relations. *Circ. Res.* 58: 755–768, 1986.
22. **Kihara, Y., W. Grossman, and J. P. Morgan.** Direct measurement of changes in intracellular calcium transients during hypoxia, ischemia, and reperfusion of the intact mammalian heart. *Circ. Res.* 65: 1029–1044, 1989.
23. **Landesberg, A., and S. Sideman.** Mechanical regulation of cardiac muscle by coupling calcium kinetics with cross-bridge cycling: a dynamic model. *Am. J. Physiol.* 267 (*Heart Circ. Physiol.* 36): H779–H795, 1994.
24. **Lee, H. C., N. Smith, R. Mohabir, and W. T. Clusin.** Cytosolic calcium transients from the beating mammalian heart. *Proc. Natl. Acad. Sci. USA* 84: 7793–7797, 1987.
25. **Marban, E., H. Kusuoka, D. T. Yue, M. L. Weisfeldt, and W. G. Wier.** Maximal Ca^{2+}-activated force elecited by tetanization of ferret papillary muscle and whole heart: mechanics and characteristics of steady contractile activation in intact myocardium. *Circ. Res.* 59: 262–269, 1986.
26. **McDonald, K. S., and R. L. Moss.** Osmotic compression of single cardiac myocytes eliminates the reduction in Ca^{2+} sensitivity of tension at short sarcomere length. *Circ. Res.* 77: 199–205, 1995.
27. **Peterson, J. N., W. C. Hunter, and M. R. Berman.** Estimated time course of Ca^{2+} bound to troponin C during relaxation in isolated cardiac muscle. *Am. J. Physiol.* 260 (*Heart Circ. Physiol.* 29): H1013–H1024, 1991.
28. **Sagawa, K.** The ventricular pressure-volume diagram revisited. *Circ. Res.* 43: 677–687, 1978.
29. **Sagawa, K., W. L. Maughan, H. Suga, and K. Sunagawa.** *Cardiac Contraction and the Pressure-Volume Relationship*. Oxford, UK: Oxford University Press, 1988, p. 1–480.
30. **Sonnenblick, E. H.** Determinants of active state in heart muscle: force, velocity, instantaneous muscle length, time. *Federation Proc.* 24: 1396–1409, 1965.
31. **Stein, R. B., J. Bobet, M. N. Oguztoreli, and M. Fryer.** The kinetics relating calcium and force in skeletal muscle. *Biophys. J.* 54: 705–717, 1988.
32. **Stennett, R. A., K. Ogino, J. P. Morgan, and D. Burkhoff.** Length-dependent activation in intact ferret hearts: study of steady-state Ca^{2+}-stress-strain interrelations. *Am. J. Physiol.* 270 (*Heart Circ. Physiol.* 39): H1940–H1950, 1996.
33. **Wood, E. H., R. L. Heppner, and S. Weidmann.** Inotropic effects of electric currents. 2. Hypotheses: calcium movements, excitation-contraction coupling and inotropic effects. *Circ. Res.* 24: 409–445, 1969.
34. **Yue, D. T.** Intracellular $[Ca^{2+}]$ related to rate of force development in twitch contraction of heart. *Am. J. Physiol.* 252 (*Heart Circ. Physiol.* 21): H760–H770, 1987.
35. **Yue, D. T., E. Marban, and W. G. Wier.** Relationship between force and intracellular $[Ca^{2+}]$ in tetanized mammalian heart muscle. *J. Gen. Physiol.* 87: 223–242, 1986.